Theor Chem Acc (2011) 128:627–638
DOI 10.1007/s00214-010-0825-4

REGULAR ARTICLE

Comparative study of the hydrolysis of a third- and a first-generation platinum anticancer complexes

Andrea Melchior · Enrique Sánchez Marcos · Rafael R. Pappalardo · José M. Martínez

Received: 14 July 2010 / Accepted: 14 September 2010 / Published online: 2 October 2010

Abstract The hydrolysis of *cis*-$[Pt(NH_3)_2Cl_2]$ (cisplatin) and of the third-generation platinum anticancer compound (*cis*-$[PtCl_2(NH_3)$-(2-picoline)] (picoplatin) has been studied quantum-mechanically using density functional theory (mPW1PW91). Due to its asymmetry, picoplatin is an interesting case, since hydrolysis may proceed through two distinct reaction paths and with the entering water molecule *sin* or *anti* to the methyl group of 2-picoline. Solvent effects were taken into account either by applying the polarizable continuum model (PCM) solvent approach or by introducing a cluster of water molecules solvating the complex. With the PCM approach, it emerges that the steric hindrance of 2-picoline has a minimum impact on the activation barriers for picoplatin hydrolysis, since the water molecule approach is far from being axial and far from the methyl group. Accordingly, the TS state geometry with 5-coordinated platinum is not significantly more distorted than in the cisplatin case. Our results point out that the use of separated reactants as reference for energy barrier gives satisfactory results for each compound and produces correct relative magnitudes of first and second hydrolysis rate constants for each compound. However, this model is not able to predict the generally faster hydrolysis experimentally observed for cisplatin with respect to picoplatin. The study of the first hydrolysis step for the two compounds in the presence of explicit water molecules shows that the entering water molecule is strongly interacting with the others through a complex hydrogen bond network. The discrete solvation model is able to correctly predict a slightly slower hydrolysis of picoplatin highlighting the need of explicit solvation to predict small differences (within an order of magnitude) in the observed rate constants.

Keywords Picoplatin · Cisplatin · DFT · Hydration · Hydrolysis · Reaction rate

Published as part of the special issue celebrating theoretical and computational chemistry in Spain.

Electronic supplementary material The online version of this article (doi:10.1007/s00214-010-0825-4) contains supplementary material, which is available to authorized users.

A. Melchior · E. Sánchez Marcos · R. R. Pappalardo · J. M. Martínez (✉)
Departamento de Química Física, Universidad de Sevilla, 41012 Sevilla, Spain
e-mail: josema@us.es

Present Address:
A. Melchior
Dipartimento di Scienze e Tecnologie Chimiche, Università di Udine, 33100 Udine, Italy

1 Introduction

Platinum-based drugs are one of the most important parts of chemotherapy treatments of a variety of malignancies. In particular, cisplatin (Scheme 1) has been employed for over 30 years in the chemotherapy of a large number of tumours [1]. The accepted mechanism of action of cisplatin consists in two stages: (1) intracellular activation by the hydrolysis of one chloride ligand, driven by the lower concentration of Cl^- anions in the cell ($\sim$3 to 20 mM) with respect to their concentration in plasma ($\sim$100 mM); (2) formation of intra-strand cross-links in DNA through the covalent binding of the Pt complex to purine bases [2, 3]. Several types of adducts can be formed; the most prevalent (most stable) is the intra-strand linkage of two adjacent guanine bases by the nitrogen atoms at position 7 (the GG adduct). The result is a bent DNA that causes the generation of defective proteins inside the cell. The cell

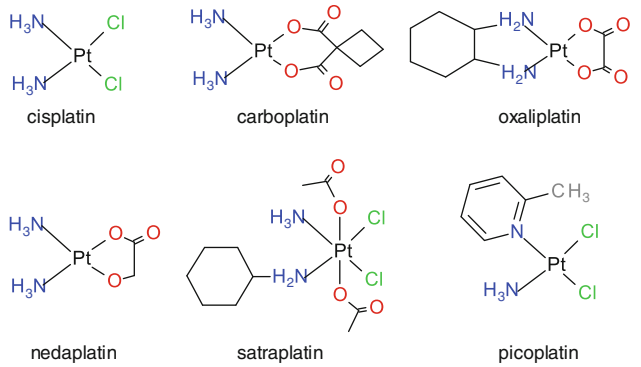

Scheme 1 Platinum anticancer compounds

tries to undo the DNA–Pt adducts and several repairing mechanisms are available to that purpose. The mechanism for DNA–Pt adduct repairing is damaged for certain types of tumour cells. Then, they cannot undo the adduct and therefore die [2, 4].

Despite the success reached by cisplatin in 30 years of clinical application, several serious side-effects (such as gastrointestinal and kidney toxicity, immune system suppression, peripheral neurotoxicity) and acquired or intrinsic resistance of tumours are still major drawbacks [2].

In order to overcome these limitations, a large number of platinum compounds have been screened in the last decades with the aim of finding new drugs with an equivalent or improved range of activity and with lower toxicity, but only three of them are currently registered for clinical use (Scheme 1): carboplatin (*cis*-diammine(1,1-cyclobutanedicarboxylato) platinum(II)), oxaliplatin (*trans*-L-1,2-diaminocyclohexaneoxalatoplatinum(II)) and nedaplatin (*cis*-diammineglycolatoplatinum(II)) [1, 4, 5].

Two other interesting compounds are currently in phase III of pharmaceutical development, namely satraplatin (bis-(acetato)-ammine-dichloro-(cyclohexylamine)platinum(IV)) and picoplatin (*cis*-amminedichloro(2-methylpyridine)platinum(II)) in Scheme 1 [5, 6]. Both compounds are particularly attractive because of milder toxicity profile, lack of cross-resistance with cisplatin, and activity in cancers non-responsive to cisplatin [7, 8].

Many theoretical studies characterized the reaction energy profiles of hydrolysis [9–20] and DNA binding [21–23] of the platinum anticancer agents in Scheme 1 in order to understand the factors involved in the effectiveness of the drug and the possibility of producing useful hints for the design of better compounds. However, theoretical comparison studies of platinum drugs reactions have not been undertaken. In previous papers, we have examined the hydration of oxaliplatin from theoretical point of view with the aid of Car-Parrinello Molecular Dynamics technique [24] and combined this information with experimental X-ray

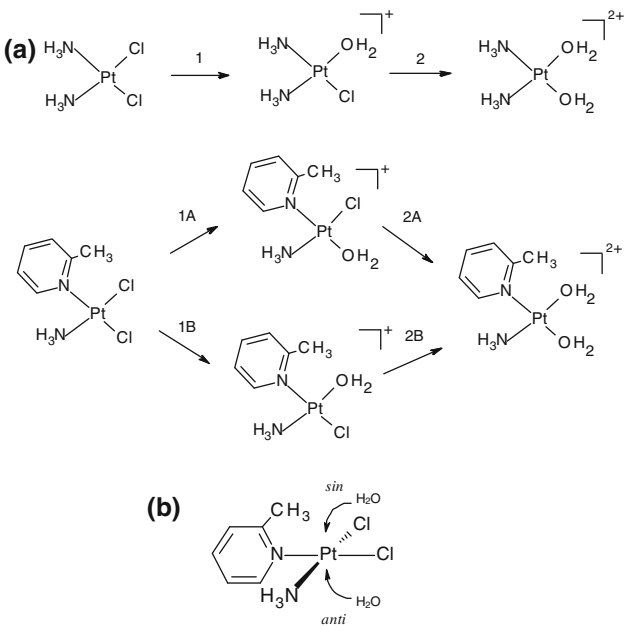

Scheme 2 **a** Cisplatin and picoplatin hydrolysis reactions; **b** stereochemistry of nucleophilic attack of water

absorption spectra, both EXAFS and XANES [25, 26], to get insight into the elucidation of its solvation structure [27].

In this paper, we present a theoretical study of chloride hydrolysis of cisplatin and picoplatin (Scheme 2), which shows a notably different chemical reactivity and pharmacological profile despite a limited structural modification, consisting in the substitution of one ammonia by 2-picoline (2-pic) as a non-leaving ligand. Steric hindrance introduced by 2-pic in picoplatin has been considered the main reason to lower the ligand substitution rate in platinum square-planar complexes, on the basis of an associative mechanism proceeding through a 5-coordinate distorted trigonal bipyramidal transition state [28]. According to this hypothesis, reaction rates for hydrolysis and picoplatin coordination to DNA bases and biological nucleophiles (e.g. glutathione) were found to proceed slower than the same for cisplatin [29]. Rate constants values of the first hydrolysis (k_1) for picoplatin [28] in *trans* and *cis* respect to 2-pic (Scheme 2a reactions 1A and 1B) are $\sim$3 times smaller than that for cisplatin obtained under similar medium conditions [30] (see Table 1), being the rate constant for the *trans* hydrolysis, k_{1A}, larger than that of the *cis* hydrolysis, k_{1B}. However, NMR data employed in Ref. [29] yield $k_{1A} < k_{1B}$ order (Table 1), apparently in contradiction with the previous finding [28], indicating that the effect of 2-pic may be not so straightforwardly interpreted. Also the experimental data for the second hydrolysis [28] are of difficult interpretation, since the order $k_{2A} > k_{2B}$ (Scheme 2a; Table 1) is unexpected according to the steric argument.

Table 1 Activation Gibbs free energy and corresponding rate constants for picoplatin and cisplatin obtained theoretically in this work along with the experimental rate constant values taken from literature

	$\Delta G^{\ddagger}$/kcal mol^{-1}	Rate constants/s^{-1}	
	Calculated	Calculated	Experimental
I hydrolysis			
Cisplatin	24.7	4.43×10^{-6}	7.59×10^{-5}[a], 7.56×10^{-5}
Picoplatin			
Path A			
sin	23.4	4.27×10^{-5}	3.19×10^{-5}[b], 5.87×10^{-6}[c]
anti	23.6	3.14×10^{-5}	
Path B			
sin	22.8	1.24×10^{-4}	2.2×10^{-5}[b], 6.87×10^{-6}[c]
anti	22.5	1.93×10^{-4}	
II hydrolysis			
Cisplatin	26.0	5.3×10^{-7}	2.5×10^{-5}[d]
Picoplatin			
Path A			
sin	23.1	6.87×10^{-5}	7.3×10^{-5}[b]
anti	23.2	5.39×10^{-5}	
Path B			
sin	23.0	8.22×10^{-5}	0.35×10^{-5}[b]
anti	23.1	6.44×10^{-5}	
Cluster reactions			
Cisplatin·15 H_2O	18.9	8.41×10^{-2}	
Picoplatin·15 H_2O	19.3	4.28×10^{-2}	

[a] Ref. [30], $T = 308$ K in 0.32 M KNO_3; second value at $T = 25$ °C in 0.1 M $HClO_4$, $\Delta H^{\ddagger} = 17.6$ kcal mol^{-1}, $\Delta S^{\ddagger} = -18.2$ cal K^{-1} mol^{-1}

[b] Ref. [28], $T = 310$ K, pH 4.6 in 0.1 M $NaClO_4$

[c] Ref. [29], $T = 296$ K pH = 6.85 (ionic medium not specified)

[d] Ref. [45], in 1 M $HClO_4$ $T = 25$ °C

In this comparative quantum-mechanical study, different approaches will be employed to take into account solvent effects: (1) reaction between the platinum complex and one water molecule in a polarizable dielectric continuum; (2) hydrolysis in presence of a cluster of 15 water molecules surrounding the platinum complex. In this way, we aim to verify to which extent 2-pic is effectively determining a higher activation barrier in hydrolysis reaction with respect to cisplatin and if such (relatively) small differences in rate constants can be theoretically predicted.

Secondly, we aim to assess the ability of DFT to predict qualitatively the hydrolysis activation barrier of a new compound (picoplatin) in relation to a reference one (cisplatin) working on the same foot. In this study, we are also interested in the examination of the use of the so-called Reactive Adduct (RA, i.e. the platinum complex plus one reactive water in the second shell) as reference for calculating the reaction barriers. This type of approach has been previously used in several works dealing with platinum drugs [14, 31, 32] and, although questioned in more recent papers [10, 13] is still employed by some authors [9].

2 Methods

Density functional theory calculations were performed with the Gaussian 03 program [33], using the mPW1PW91 functional [34]. Geometry optimizations were carried out in vacuum and with a 6-31+G(d) basis set for all atoms except the platinum atom, which was described by the quasi-relativistic Stuttgart–Dresden pseudopotential [35] (denoted Small Basis, SB).

Improved energies were obtained by single point calculations at the equilibrium geometries using a large basis (LB) consisting of a 6-311++G(3df,2pd) basis sets for all elements, but platinum which was described by the Stuttgart–Dresden pseudopotential augmented by a set of diffuse ($\alpha_s = 0.0075$, $\alpha_p = 0.013$, $\alpha_d = 0.025$) and polarization functions ($\alpha_f = 0.98$) for the valence orbitals [36].

In order to confirm that stationary points were actually minima or transition state geometries, the analytical calculation of second derivatives of the energy and vibrational frequency analysis were carried out. Potential energy profiles were estimated from total electronic energies with the SB and LB sets and adding zero point energy (ZPE) and thermal corrections at 298.15 K.

As already mentioned, solvent effects were taken into account by two alternative ways: (1) implicit solvent introduced by the PCM method [37] using the universal force field (UFF) [38] radius for the spheres centred on each atom (energy calculations were carried out without re-optimization); (2) discrete solvation defined by 15 water molecules surrounding the platinum complex. In the last case, the large computational effort associated to

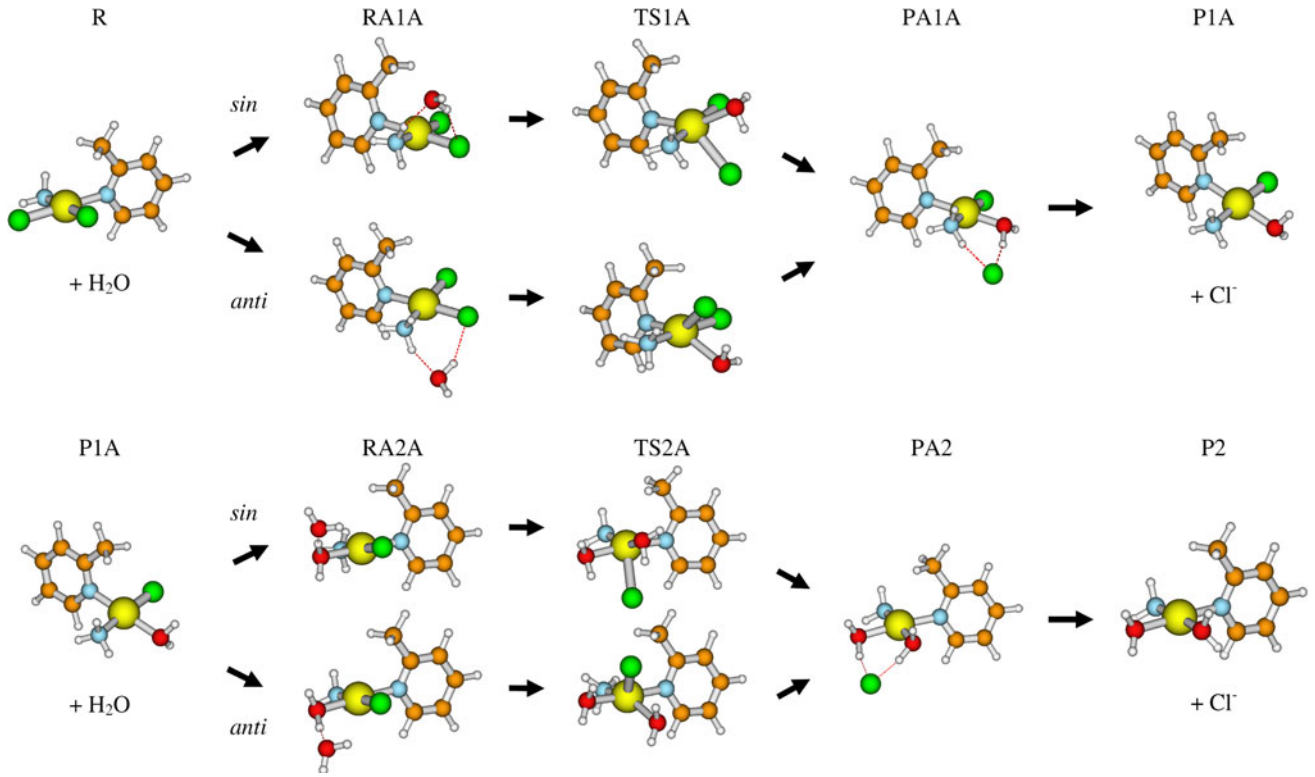

Fig. 1 Optimized structures for the hydrolysis of picoplatin according to path A in Scheme 2

the number of water molecules inserted in the cluster limited the comparative study to the first hydrolysis process.

We considered separated reactants (R) to define the energy reference state in order to predict the activation barriers despite several works which consider the reactant adducts (RA in Figs. 1, 2, 3, 4) as Refs. [14, 31, 32]. The consideration of only a single reacting water molecule hydrogen-bonded to the complex (i.e. in the second coordination shell in the vicinity of the metal) has been criticized by some authors [10, 13] for neglecting water–water interactions. This is not the case when an explicit solvation approach is used and an enough number of water molecules are present in the model system, thus we choose the complex–water cluster as reference.

Rate constants have been calculated by means of the Eyring equation:

$$k = \frac{k_B T}{h} e^{-\frac{\Delta G^{\ddagger}}{RT}}$$

The activation Gibbs' free energy $\Delta G^{\ddagger}$ value has been calculated by the individual Gibbs free energy values obtained using the LB in solvent with the separate reactants as reference. To calculate the activation Gibbs free energies in solution, the entropic translational term calculated in gas-phase was not taken into account.

3 Results and discussion

Reactions studied in this work are reported in Scheme 2. On the basis of a large number of experimental data, it is widely accepted that the hydrolysis of the platinum(II) anticancer complexes (Scheme 2a) is a bimolecular nucleophilic substitution (S_N2). The initial square-planar complex is converted to a bipyramidal (5-coordinated) transition state (TS) in which the incoming water molecule and the leaving chloride are weakly bound to the metal. The structural features of this trigonal bipyramid are relevant for determining the hydrolysis activation barrier.

In contrast to cisplatin, picoplatin presents two paths (Scheme 2) for the chloride substitution: (A) a first hydrolysis of the chloride ligand in *trans* position to the 2-picoline group followed by a second hydrolysis where the replacement of the *cis* chloride ligand by a water molecule takes place; (B) the hydrolysis processes occur in the reversed sequence, i.e. the *cis* chloride substitution precedes the *trans* one. The individual rate constants, determined by NMR [28] (Table 1), indicate that the first aquation in picoplatin occurs slightly slower than the second when the reaction proceeds through path A ($k_{1A} < k_{2A}$) while the opposite is found in path B ($k_{1B} > k_{2B}$).

A more subtle mechanistic feature of this picture may emerge from the fact that 2-pic defines two possible sides

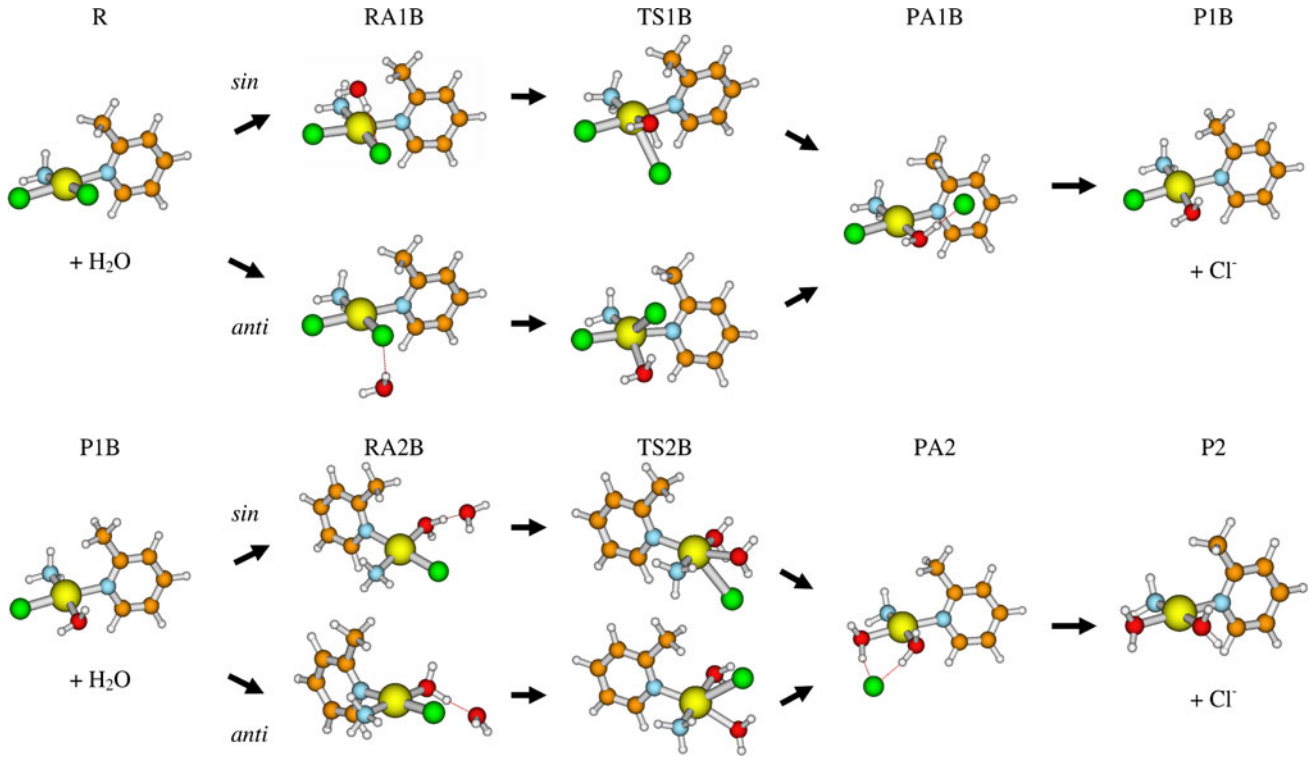

Fig. 2 Optimized structures for the hydrolysis of picoplatin according to path B in Scheme 2

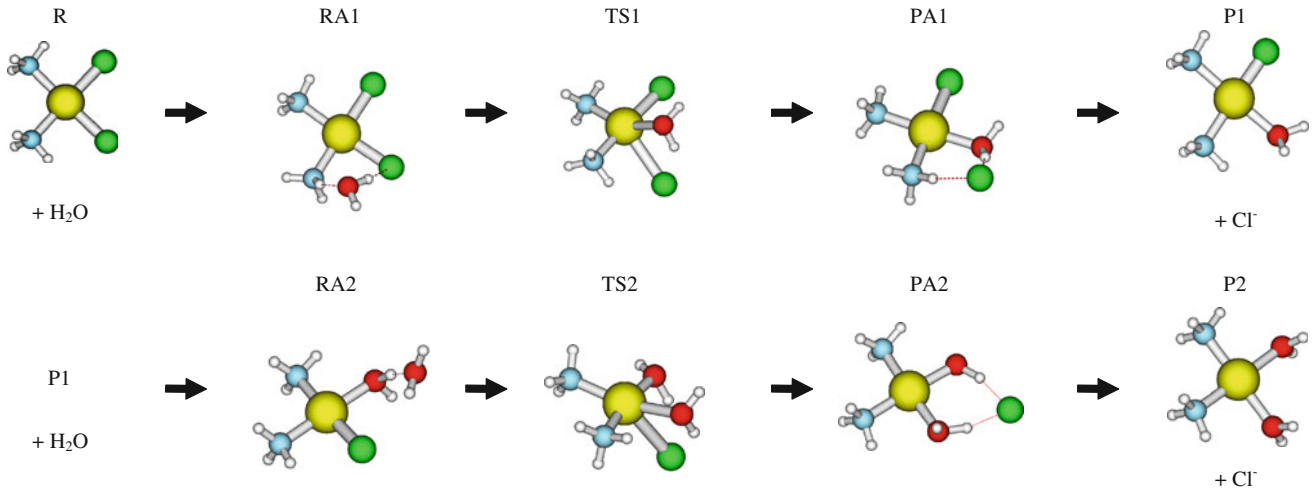

Fig. 3 Structures of cisplatin reactants, transition states and products for the two-step hydrolysis process

for nucleophilic attacks: one *sin* and one *anti* with respect to the orientation of the methyl group leading to two possible TS for each reaction path (Scheme 2b). The importance of the methyl position is also suggested by the relative magnitude of the experimental rate constants ($k_{3\text{-pic}}/k_{2\text{-pic}}$), which are mostly higher when 2-picoline is replaced by 3-picoline ($k_{3\text{-pic}}/k_{2\text{-pic}} \sim 1.4$ to 4.7 and 0.5–22 for reaction 1 and 2, respectively) [28]. This experimental finding compelled us to study the reaction proceeding through TS with both water approaches with respect to the methyl group.

The optimized structures of picoplatin and cisplatin complexes with one explicit water molecule (reactants, transition states and products) are displayed for the two-step hydrolysis reaction in Figs. 1, 2, 3. Selected geometrical parameters are reported in Tables 2, 3, 4. Picoplatin complexes have been designated as follows: R, reactant complex; RA, reactant adduct labelled with the reaction

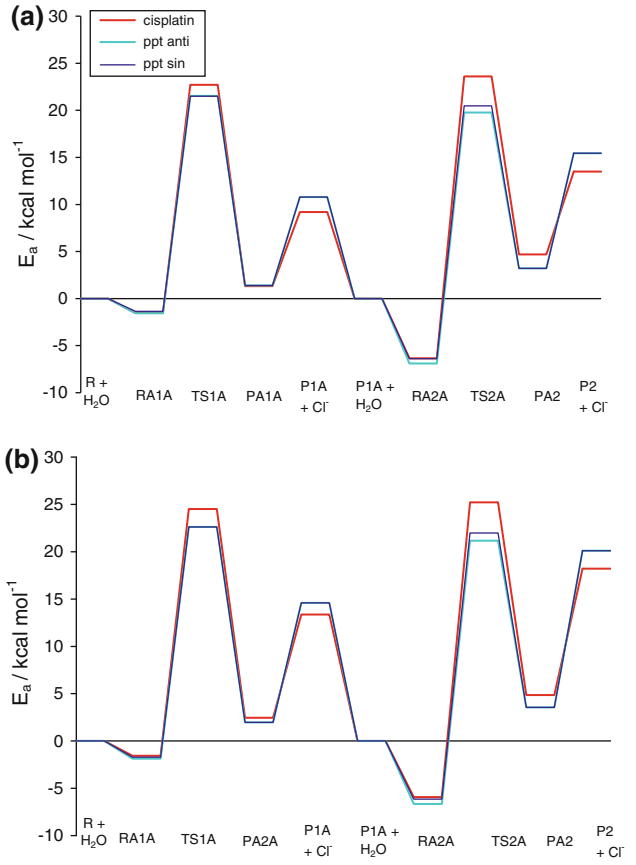

Fig. 4 Activation energy profile for the hydrolysis of cisplatin and picoplatin (*ppt*) through path A (see Sect. 2 for details): **a** small basis set; **b** large basis set. For better comparison, the profile for cisplatin is also reported

number (1,2) followed by specific path (A,B) as displayed in Scheme 2: TS transition state; PA product adduct; P product complex. Note that, only one PA for each reaction has been considered, since on the basis of preliminary calculations minimal differences in energy between local minima of products were found.

The theoretical picoplatin and cisplatin geometries are in good agreement with available crystal structures as expected on the basis of the good results of the mPW1PW91 functional in predicting platinum(II) complexes geometries [39]. For picoplatin and cisplatin, deviations smaller than 0.015 Å from crystal structures [28, 40, 41] are found for Pt–Cl bond distances, while the average deviation on the Pt–ligand distances remains smaller than 0.03 Å for both compounds. It should also be noted that two isomers of picoplatin, defined by the rotation of the methyl group of 2-pic have been isolated in solid state [28, 41]. Variable temperature ^{1}H-NMR experiments [42] suggested a moderately slow equilibrium (broad resonance of the methyl group) between the two forms on the NMR timescale which becomes fast at $T > 300$ K (sharp resonance). For simplicity, in this study, we will consider only one of the two possible isomers (Figs. 1, 2).

3.1 First hydrolysis

In path A, the formation of the RA1A results in a slight stabilization of the system (Table S1; Fig. 4) with respect to the separate reactants due to the weak interaction of water with ammonia and chloride. The *sin* and *anti* isomers are nearly isoenergetic ($\Delta E = 0.2$ kcal mol^{-1}) thus indistinguishable at room temperature.

In the 5-coordinated TS1A (Fig. 1), the entering (water) and leaving chloride ligand form a wide angle with platinum and the third atom in the trigonal equatorial plane (O_w–Pt–$N_{2\text{-pic}}$ and Cl–Pt–$N_{2\text{-pic}}$ are 150/152° and 141/139°, Table 2) similar to those found for cisplatin TS (151 and 140°, Table 4; Fig. 3). This shows that no important geometrical distortion of the TS is present in picoplatin with respect to the reference compound. Then, it is worth underlying that the entering water molecule does not follow an axial channel, but rather a tilted approach line (~40° with respect to the molecular plane).

The activation energy (E_a) calculated with the SB is equal to 21.5 kcal mol^{-1} when considering both *sin* and *anti* TS1A compounds (Table S1; Fig. 4a), indicating that no preferential side for nucleophilic attack is determined by the orientation of the methyl group. When the LB is used the barrier slightly rises, as generally found, and again no differences are observed between the *sin* and *anti* transition states ($E_a = 22.6$ kcal mol^{-1}, Fig. 4b) as well. The E_a for this process is lower than that found for the first hydrolysis of cisplatin (22.7 and 24.5 kcal mol^{-1} with SB and LB, respectively, Table S1; Fig. 4) and the calculated rate constant results in a faster hydrolysis for picoplatin (Table 1).

If path B is considered, i.e. first hydrolysis occurring in *cis* to 2-pic, the formation of RA1B complexes is an endothermic process, regardless the basis sets employed (Table S1; Fig. 5). This result casts some doubts on the physical meaning of taking the optimized supermolecule, i.e. the complex plus one water molecule, as reference for the E_a calculation. This is in agreement with Lau and Deubel's results [13] who find that the formation of the RA is not thermodynamically favoured (positive ΔG^0 of formation) in the presence of a dielectric continuum, as well as that the reactivity of cisplatin can be similarly explained without the introduction of the RA. Its absence as intermediate step from reactants to TS is also suggested by ab initio MD simulations which did not give evidence its formation in the presence of a significant number of water molecules [19].

As in the previous cases, the *sin* and *anti* isomers are nearly equal in energy ($\Delta E = 0.4$–0.5 kcal mol^{-1}, Table

Table 2 Relevant bond distances and angles in picoplatin complexes involved in path A

Path A	(1)							(2)					
	R	RA1A		TS1A[a]		PA1A	P1A	RA2A		TS2A[b]		PA2	P
		anti	*sin*	*anti*	*sin*			*anti*	*sin*	*anti*	*sin*		
Bond (Å)													
Pt–X_l	2.315	2.329	2.330	2.741	2.748	3.871	–	2.305	2.304	2.740	2.694	3.651	–
Pt–X	2.309	2.314	2.313	2.319	2.320	2.319	2.288	2.089	2.090	2.102	2.096	2.057	2.123
Pt–$N_{2\text{-pic}}$	2.054	2.044	2.043	2.021	2.023	2.014	2.000	2.011	2.011	2.001	2.004	2.023	2.005
Pt–N_{am}	2.095	2.091	2.092	2.077	2.076	2.078	2.104	2.093	2.094	2.069	2.077	2.051	2.034
Pt–O_w(ent)	–	3.639	3.600	2.436	2.438	2.058	2.123	3.711	3.715	2.367	2.355	2.069	2.106
Angle (deg)													
O_w(ent)–Pt–N_t	–	119	120	150	152	179	177			155	156	174	–
X_l–Pt–$N_{2\text{-pic}}$	178	178	179	141	139	134	–	177	177	135	131	175	176
X–Pt–N_{am}	178	179	179	176	176	176	176	178	179	176	174	125	178
Dihedral (deg)													
N_{am}–Pt–$N_{2\text{-pic}}$–C_2	102	104	99	105	102	105	100	100	97	87	77	75	93

See also Fig. 1 (X_l leaving chloride, X spectator group (second chloride in first reaction, water in the second), $N_{2\text{-}pic}$ pyridine nitrogen, N_{am} ammonia nitrogen, N_t nitrogen *trans* to leaving group, O_W(ent) entering water oxygen, C_2 carbon 2 in 2-pic)

[a] TS1A imaginary frequency eigenvalues: TS(*anti*) = 169i cm^{-1}, TS (*sin*) = 167i cm^{-1}

[b] TS2A imaginary frequency eigenvalues: TS(*anti*) = 181i cm^{-1}, TS (*sin*) = 179i cm^{-1}

Table 3 Relevant bond distances and angles in picoplatin complexes involved in path B

Path B	(1)							(2)					
	R	RA1B		TS1B[a]		PA1B	P1B	RA2B		TS2B[b]		PA2	P
		anti	*sin*	*anti*	*sin*			*anti*	*sin*	*anti*	*sin*		
Bond (Å)													
Pt–X_l	2.309	2.318	2.316	2.784	2.738	4.035	–	2.313	2.315	2.737	2.735	3.651	–
Pt–X	2.315	2.319	2.321	2.321	2.321	2.314	2.297	2.076	2.081	2.085	2.091	2.057	2.123
Pt–$N_{2\text{-pic}}$	2.054	2.053	2.050	2.047	2.047	2.055	2.069	2.063	2.057	2.030	2.028	2.023	2.005
Pt–N_{am}	2.095	2.086	2.089	2.066	2.069	2.059	2.030	2.042	2.040	2.034	2.029	2.051	2.034
Pt–O_w(ent)	–	3.468	3.453	2.347	2.376	2.033	2.099	3.776	3.657	2.320	2.374	2.069	2.106
Angle (deg)													
O_w(ent)–Pt–N_t	–	112	113	154	156	177	174	123	121	157	160	174	–
X_l–Pt–$N_{2\text{-pic}}$	178	178	177	139	135	61	–	178	179	133	132	125	178
X–Pt–N_{am}	178	178	179	176	177	179	177	178	178	172	173	175	176
Dihedral (deg)													
N–Pt–$N_{2\text{-pic}}$–C_2	102	95	83	72	94	82	78	87	107	104	92	75	93

See also Fig. 2 (X_l leaving chloride, X spectator group (second chloride in first reaction, water in the second), $N_{2\text{-}pic}$ pyridine nitrogen, N_{am} ammonia nitrogen, N_t nitrogen *trans* to leaving group, O_W(ent) entering water oxygen, C_2 carbon 2 in 2-pic)

[a] TS1B imaginary frequency eigenvalues: TS(*anti*) = 189i cm^{-1}, TS (*sin*) = 193i cm^{-1}

[b] TS2B imaginary frequency eigenvalues: TS(*anti*) = 158i cm^{-1}, TS (*sin*) = 171i cm^{-1}

S1) supporting the hypothesis that there is no preferential side for the nucleophilic attack. The angles formed by water and chloride with ammonia nitrogen are still far from those of an equilateral triangle (O_w–Pt–N_{am} = 154/156° and Cl–Pt–N_{am} = 139/135°, Table 3) and slightly more distorted than those found for structures of path A and in the case of cisplatin. It is noticeable that in TS1B the dihedral angle N_{am}–Pt–$N_{2\text{-pic}}$–C_2 (72–94°, Table 3) is smaller than that found in the TS of path A (105–102°, Table 2). This arrangement minimizes the repulsive interaction between the methyl group and the equatorial entering/leaving ligands.

Table 4 Relevant bond distances and angles in cisplatin

	R1	RA1	TS1[a]	PA1	P1	RA2	TS2[b]	PA2	P2
Distance (Å)									
Pt–X_l	2.308	2.321	2.755	3.900	–	2.294	2.733	3.761	–
Pt–X	–	2.313	2.315	2.315	2.284	2.112	2.086	–	–
Pt–N_t		2.081	2.064	2.049	2.031	2.098	2.082	2.59	–
Pt–N_c	2.092	2.090	2.076	2.080	2.107	2.024	2.030	–	2.035
Pt–O_w(ent)	–	3.659	2.395	2.048	2.104	3.765	2.307	2.054	2.101
Angle (deg)									
O_w(ent)–Pt–N	–	122	151	177	176	121	158	178	179
X_l–Pt–N_t	83	178	140	138	–	176	133	131	–
X_l–Pt–N_c	–	85	75	50	–	88	100	–	–

X_l leaving group, X spectator group (second chloride in first reaction, water in the second), $N_{c/t}$ nitrogen *cis/trans* to leaving group

[a] TS1 imaginary frequency eigenvalues: TS(*anti*) = 193i cm^{-1}

[b] TS2 imaginary frequency eigenvalues: TS(*anti*) = 188i cm^{-1}

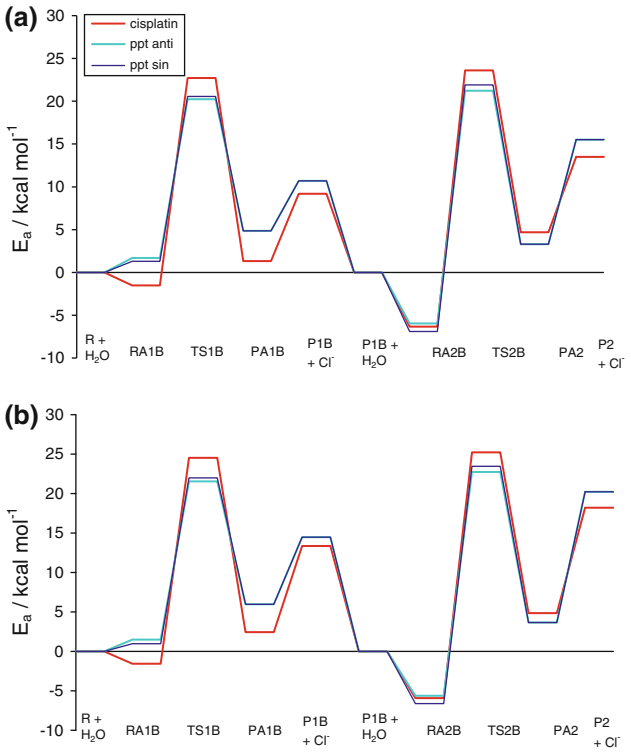

Fig. 5 Activation energy profile for the hydrolysis in water of cisplatin and picoplatin (*ppt*) through path B (see Sect. 2 for details): **a** small basis set; **b** large basis set

In this case, the E_a calculated with the SB is equal to 20.2 and 20.6 kcal mol^{-1} for the *anti* and *sin* TS1B compounds, respectively (Table S1; Fig. 5a), indicating that a slightly faster reaction occurs following the first path. With LB this small energy difference holds up (E_a = 21.5 and 22 kcal mol^{-1} Table S1; Fig. 5b). The calculated E_a is lower than that of cisplatin and also for the *trans* reaction which would correspond to a faster rate at this site (Table 1). The introduction of the implicit solvent model is responsible of this trend, as evidenced by comparing with the corresponding activation barriers in vacuum (not reported).

In summary, the results for the first hydrolysis would predict a faster reaction for picoplatin with respect to cisplatin which disagrees with the rate constant trend observed in the NMR experiments [28]. The *cis/trans* activation barrier difference is similar (E_a(path A) − E_a(path B) = 0.6 − 1.1 kcal mol^{-1} with LB) in agreement with similar reaction rates calculated from NMR indicating that the steric hindrance of 2-pic is not a main factor in the determination of the reaction rate constant.

3.2 Second hydrolysis

All monoaqua complexes form adducts (RA2A in Fig. 1, RA2B in Fig. 2 and RA2 in Fig. 3) with the entering water molecule interacting via hydrogen bond with one chloride and the already coordinated water molecule. The stabilization of the system with respect to separate reagents is higher than that found in reaction 1 and a small energy difference is observed when cisplatin profile is compared with the picoplatin one, since all relative energy values lie in the range of 1 kcal mol^{-1} (Table S1; Figs. 4, 5).

Transition state structures for picoplatin (TS2A in Fig. 1 and TS2B in Fig. 2) are characterized by the fact that the entering and leaving groups form a distorted triangle with the non-leaving ligand in the equatorial plane, the values of the angles formed with the nitrogen atom are close to those found for cisplatin TS (Tables 2, 3, 4). For example, the O_w–Pt–N_t and Cl–Pt–N_t in TS2A are 155/156° and 135/131°, respectively, while in cisplatin TS their values are 158 and 133°. The rotation of 2-pic is a feature of *cis* hydrolysis since the N_{am}–Pt–$N_{2\text{-pic}}$–C_2 dihedral in TS2A

(77/87°) is smaller than in the TS2B (104/92°), as already observed in reaction 1 for TS1B and TS1A.

The E_a calculated with the SB is equal to 19.8 and 20.5 kcal mol^{-1} (21.2 and 22.0 kcal mol^{-1} with LB, see Table S1; Fig. 4) when considering the *anti* and *sin* TS2A compounds, indicating a light preference for the *anti* nucleophilic attack. The same preferred side is found for TS2B where E_a calculated with SB is 21.2 and 21.9 kcal mol^{-1} (22.7 and 23.5 kcal mol^{-1} with LB, Fig. 5) for *anti* and *sin* paths, respectively.

According to the results, only minimal differences in reaction rates can be attributed to the steric hindrance introduced by the ligand 2-pic, since the nucleophilic attack is far from being axial. Both entering and leaving ligands form wide O–Pt–N angles when the substitution occurs *trans* to 2-pic (TS1A, TS2B in Figs. 1, 2), and therefore they keep far from the methyl group. When the reaction in *cis* to 2-pic is considered (TS2A in Fig. 1 and TS1B in Fig. 2), the steric hindrance is minimized by the rotation around N_{am}–Pt–$N_{2\text{-pic}}$–C_2 dihedral angle (Tables 2, 3). However, it is reasonable to consider that the steric hindrance of 2-pic may become important when the nucleophile is larger than water, such as glutathione (a tripeptide considered to be one of the factors of deactivation of platinum-based antitumour agents) or guanosine-5′-monophosphate [29]. The very slow substitution reactions with these two nucleophiles were proposed to play a major role in determining the activity of picoplatin against cisplatin-resistant cell lines [29]. In addition, recent studies on other platinum-based drugs suggested a major role of the steric hindrance of the non-leaving ligands both in determining the binding to metallothioneins [43] and on the formation of the interstrand cross-links [44], therefore determining their biological activity.

According to our findings, it can be predicted that for path A the second reaction step is faster than the first one ($\Delta E_a = E_a(1) - E_a(2) = +1 - +1.7$ kcal mol^{-1}) while the reverse is found for path B ($\Delta E_a = -1 - -1.5$ kcal mol^{-1}). The calculated $\Delta G^{\ddagger}$ and rate constants (Table 1) for the substitution of the chloride *trans* to ammonia agrees with experimental findings for picoplatin ($k_{1A} < k_{2A}$ and $k_{1B} > k_{2B}$, see Table 1). When cisplatin is considered, the calculated E_a for second hydrolysis (23.6 and 25.2 kcal mol^{-1} with SB and LB, respectively, Table S1) is about 1 kcal mol^{-1} higher than the value for first hydrolysis, thus predicting a slower second hydrolysis, in agreement with experimental dissociation rate constants in acidic conditions [30, 45].

It should be also noted that if the E_a would be referred to the RA complexes the experimental trends of the rate constants of each species would not be reproduced. This result is not achieved in a recent study on picoplatin [9], when the RA with a single water molecule is taken as reference. In the same study, when two additional water molecules were introduced a correct k_1/k_2 order in each single reaction path is found [9], but the k_1 and k_2 constants differ by several orders of magnitude (up to 5), far from the experimental observations that indicate a factor <20 (Table 1). This overestimation of rate constant gap may be due to the choice of RA as reference.

In summary, we can conclude that whereas the behaviour of each compound is reasonably described by the model used here, the generally higher hydrolysis rate of cisplatin with respect to picoplatin is not predicted, even qualitatively, on the basis of the E_a values found.

3.3 Hydrolysis model with explicit water molecules

To obtain a reasonable description of the close hydration structure of cisplatin, a large number of explicit water molecules should be supplied, since from recent statistical simulations hydration numbers in the range 13–19 have been found for cisplatin [46, 47].

A cluster composed by the platinum complex and 15 water molecules has been used as model for chloride hydrolysis. With this number of water molecules, it is still possible to carry out optimizations and follow the reaction coordinate without lowering the level of theory used in the previous section. For computational reasons, this kind of approach has been only applied to the first hydrolysis reaction, and in the case of picoplatin to the exchange ligand reaction of the chloride *trans* to 2-pic. Anyway, the study of the first hydrolysis process remains important since in these cisplatin-like complexes, the monohydrated species rather than the dihydrated species is believed to bind to DNA [29]. Furthermore, NMR experiments for picoplatin evidenced that the *trans* mono aqua species reacts much faster with DNA than the *cis* one [48].

The optimized structures of Reactant (R15), TS (TS15) and Product (P15) are shown in Fig. 6 with some relevant structural parameters collected in Table 5. Different hydration of the two platinum complexes are observed: whereas cisplatin is completely surrounded by the hydration shell, the substitution of an ammonia with 2-pic breaks the hydration in picoplatin favouring a preferential solvation of the rest of the complex.

If the reactant structures (R15 in Fig. 6) are compared to RA1A (Fig. 1) and RA1 (Fig. 3), the Pt–Cl bonds (Tables 2, 4, 5) become longer with the inclusion of specific solute–water interactions (Δ(R15 − RA) = +0.065 Å and +0.039/0.058 Å for cisplatin and picoplatin, respectively). Note that for the latter the bond elongation is lower for the Pt–Cl bond *trans* to 2-pic. On the contrary, Pt–N(amine) bonds become shorter (Δ(R15 − RA) = −0.043 and −0.046 Å for cisplatin and picoplatin, respectively). The Pt–$N_{2\text{-pic}}$ bond is much less affected being Δ(R15 − RA1) only equal to −0.005 Å. When the TS15 structures are compared

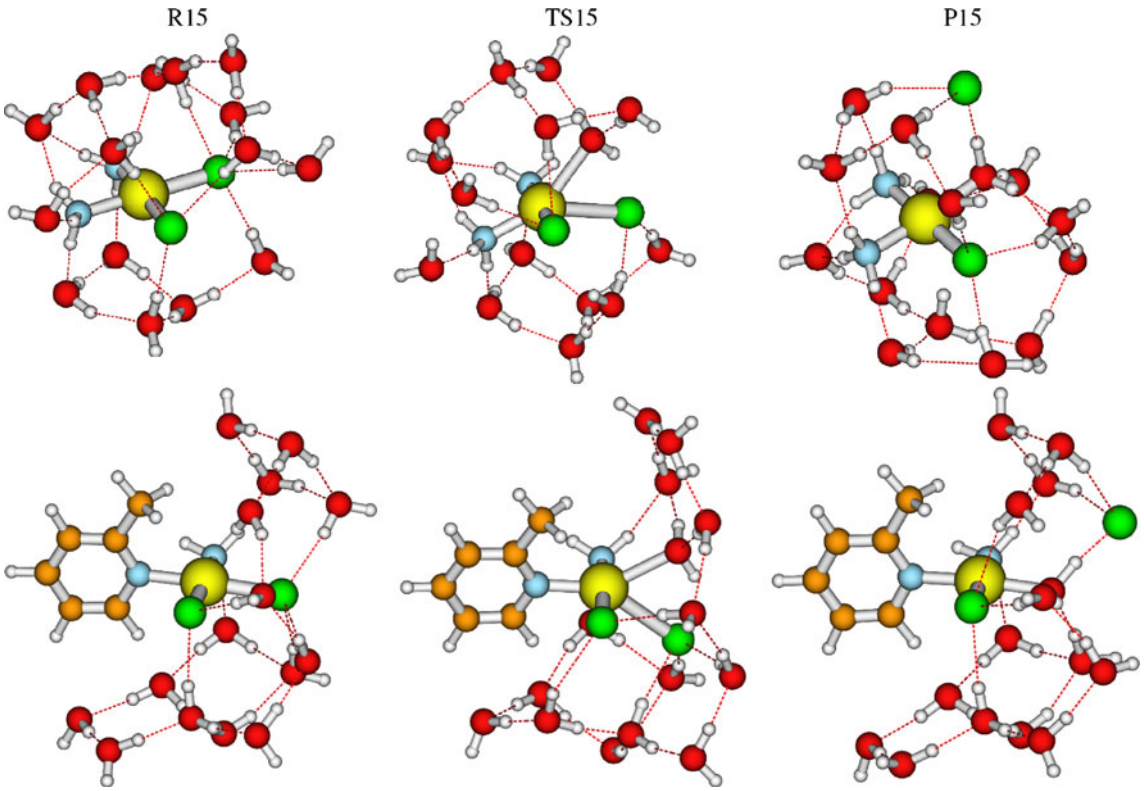

Fig. 6 Optimized structures of cisplatin and picoplatin with 15 water molecules

Table 5 Relevant bond distances and angles in cisplatin and picoplatin complexes optimized in presence of 15 explicit water molecules

	Cisplatin			Picoplatin		
	R	TS[a]	P1A	R	TS[b]	P1A
Bond (Å)						
Pt–Cl_l	2.394	2.839	3.900	2.369	2.837	4.376
Pt–Cl	2.370	2.353	2.380	2.372	2.354	2.378
Pt–N_t	2.039	2.023	2.025	2.024	2.007	2.006
Pt–N_{am}	2.046	2.050	2.040	2.046	2.053	2.039
Pt–O_w(ent)	–	2.633	2.108	–	2.496	2.087
Angle (deg)						
O_w(ent)–Pt–N_t	–	153	176	–	149	175
X_l–Pt–N_t	177	142	131	177	145	153
X–Pt–N	178	177	178	177	177	178

See also Fig. 6 (Cl_l leaving chloride, *Cl* spectator chloride, $N_{2\text{-}pic}$ picoline nitrogen, N_{am} ammonia nitrogen, N_t nitrogen *trans* to leaving group, O_W(ent) entering water oxygen; C_2 carbon 2 in 2-picoline)

[a] Cisplatin TS imaginary frequency eigenvalue: TS(*anti*) = 151i cm^{-1}

[b] Picoplatin TS imaginary frequency eigenvalue: TS(*anti*) = 145i cm^{-1}

to TS1A (Fig. 1) and TS1 (Fig. 3), again the Pt–Cl_l and Pt–Cl bonds are lengthened by the specific hydration included (Δ(TS15 − TS1) = +0.083/+0.038 and +0.092/+0.034 Å for cisplatin and picoplatin, respectively) while the Pt–N_t and Pt–N_{am} bonds shorten their distances (Δ(TS15 − TS1) = −0.041/−0.026 and −0.015/−0.024 Å for cisplatin and picoplatin). However, the most remarkable difference with respect to the complexes with a single water is found for the Pt–O_w(ent) bond (Δ(TS15 − TS1) = +0.238 and +0.059 Å for cisplatin and picoplatin) which reveals the large effect caused by the introduction of a large number of explicit water molecules on cisplatin TS15 structure. Accordingly, in TS15 structures of picoplatin and cisplatin (Table 5), the Pt–Cl_l bonds are similar (Δ = (cisplatin − picoplatin) = 0.002 Å) whereas the Pt–O_w(ent) bond is much longer in cisplatin (Δ = +0.137 Å). This is not observed in the analogue TS1A and TS1 species (Tables 2, 4) but rather the opposite trend is found (Δ = −0.042 Å) for Pt–O_w(ent) bond. On the contrary, the Pt–Cl_l bonds remain similar (Δ = 0.01 Å). The angles formed by the water and the chloride ligands with the *trans* nitrogen are similar for the two complexes (O_w(ent)–Pt–N_t = 153° and Cl_l–Pt–N_t = 142° for cisplatin and 149 and 145° for picoplatin) and not far from the same parameters measured in the structures of path A (Table 2) and in cisplatin (Table 4). Therefore, the introduction of 15 explicit water molecules does not drastically affect the arrangement of the equatorial plane of the transition states, while causes modifications of the bond distances (shorter Pt–N and longer Pt–Cl) and sets a clear

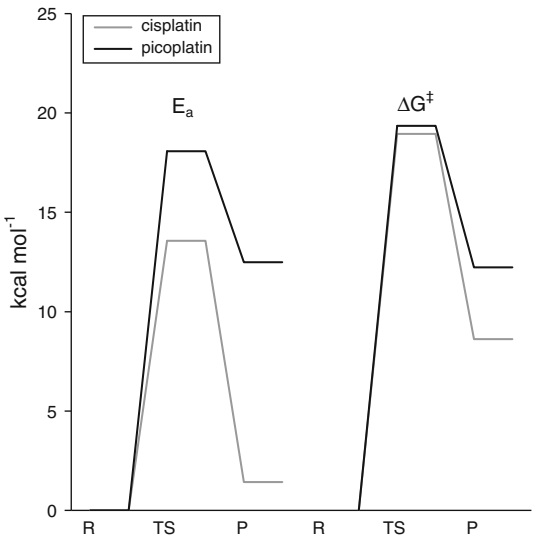

Fig. 7 Activation energy (E_a) and Gibbs free energy ($\Delta G^{\ddagger}$) profiles for the hydrolysis of first chloride in the platinum complexes with 15 water molecules. In the case of picoplatin, the leaving group is the Chloride *trans* to $N_{2\text{-pic}}$

differentiation of the Pt–O_w(ent) bond in TS15 structures of cisplatin and picoplatin. This suggests that the markedly different hydration structure of the complex is important in modifying the TS structure and therefore the ligand exchange mechanism.

The analysis of TS15 structures and of IRC paths shows that in both complexes the entering water proceeds from an intermediate equatorial/axial position quite tilted with respect to the axis passing through platinum and perpendicular to the plane of the complex (i.e. far from the methyl in the case of picoplatin). The water molecules distributed on the top and bottom of the complex re-arrange minimally their positions in the progress of the reaction, while those directly bonded to the entering one are more perturbed. It is now evident that the "reactive" water molecule is hydrogen-bonded to the leaving chloride and to two additional water molecules embedded in a complex bonding network. This suggests that cooperative effects due to the ensemble of water molecules are intimately joined to the reaction coordinate. Therefore, the use of the RA complex as reference energy for the reaction energy profile and continuum models to represent the solvation contribution may be unsuitable to compare small differences in activation barriers as specific water–water interactions are neglected.

The calculated E_a for cisplatin (13.6 kcal mol^{-1}, see Fig. 7) is lower than $\Delta H^{\ddagger}$ obtained experimentally (17.6 kcal mol^{-1}) [30] while $\Delta S^{\ddagger}$ (−17.8 cal mol^{-1} K^{-1}) is similar to the experimental one (−18.3 cal mol^{-1} K^{-1}) [30]. In the case of picoplatin E_a is 18.1 kcal mol^{-1} (>than cisplatin), as expected on the basis of the shorter bond of the leaving group with respect to cisplatin ($\Delta = 0.02$ Å, Table 5), while the corresponding $\Delta G^{\ddagger}$ is only 0.4 kcal mol^{-1} higher (Fig. 7). This result implies a smaller activation entropy ($\Delta S^{\ddagger} = -4.0$ cal mol^{-1} K^{-1}) for picoplatin. The calculated rate constants are 2–3 orders of magnitude higher than the experimental ones, but their relative value is similar (within 1 order of magnitude).

4 Conclusions

A comparative study of the hydrolysis for two current antitumoural complexes has been carried out in this work by calculating reaction energy profiles at the same level of theory and applying the same solvation models. The computational level is shown to be appropriate for describing the structure of the two complexes, with a good agreement with experimental structures.

The use of the RA as reference compound to define the profile is shown to be a controversial choice, since, in this case, the optimization in gas-phase leads to the first water molecule to interact with any group able to form hydrogen-bonding, thus creating a situation which is not realistic in aqueous solution. This is supported by the optimized structure of the hydrated complex at the same level of theory, which shows that any water molecule interacting with a single ligand of the platinum complex is always bound to one or two additional water molecules.

The fact that the RA approach gives sometimes reasonable results could be due to the fact that additional water–ligand interactions partially compensate the missing water–water ones. This implies that choosing various local minima (which lie all within few kcal mol^{-1}) makes possible to reproduce experimental trends. The approach where the separate reagents are considered as reference seems to reproduce in a satisfactory way the relative k_1/k_2 values for cisplatin or picoplatin and makes unnecessary the use of the RA. Furthermore, if the RA was taken as reference we would not be able to reproduce the relative k_1/k_2 ratio in the two hydrolysis paths of picoplatin. A much higher activation barrier (several kcal mol^{-1}) for the second hydrolysis of cisplatin would be obtained, which is actually found to proceed only slightly slower [45] than the first hydrolysis, predicted on the basis of the value calculated respect to the separate reagents.

In general, this way to estimate the rate constants leads to predict much faster reactions for picoplatin than for cisplatin (∼2 orders of magnitude of k_1) [9], which does not agree with the experimental results. These findings, along with the coherence of the description of picoplatin hydrolysis, indicate that the steric hindrance of the 2-pic in picoplatin is only marginally influencing the hydrolysis rate according to this model. These results indicate that this

type of quantum chemical models are not enough to predict, at least qualitatively, the reactivity of cisplatin derivatives with respect to the reference compound.

On the contrary, the use of clusters with a significant number of water molecules leads to a k_1 value which is qualitatively consistent (Table 1) with the relative picoplatin/cisplatin reaction rates and shows that 2-pic is drastically modifying the hydration structure, leaving less water molecules interacting with the complex. Contrary to what found using the representation with one water molecule only, a stronger Pt–Cl_l bond in the reactant structure of picoplatin is calculated justifying the slower reaction rate with respect to cisplatin. Within this view, we believe that further studies with a more complete description of outer solvation shells, helped by the introduction of dynamic factors, could be very useful for the interpretation of ligand exchange mechanisms as pointed out by Carloni et al. [19].

Acknowledgments We acknowledge Spanish "Ministerio de Ciencia y Innovación" for the financial support (project number CTQ2008-05277) and "Programa de movilidad de jovenes doctores" (SB2009-0081).

References

1. Kelland L (2007) Nat Rev Cancer 7:573–584
2. Bloemink MJ, Reedijk J (1996) Met Ions Biol Syst 32:641–685
3. Jamieson ER, Lippard SJ (1999) Chem Rev 99:2467–2498
4. Todd RC, Lippard SJ (2009) Metallomics 1:280–291
5. Shah N, Dizon DS (2009) Future Oncol 5:33–42
6. Teicher BA (2008) Clin Cancer Res 14:1610–1617
7. Choy H, Park C, Yao M (2008) Clin Cancer Res 14:1633–1638
8. Eckardt JR, Bentsion DL, Lipatov ON, Polyakov IS, MacKintosh FR, Karlin DA, Baker GS, Breitz HB (2009) J Clin Oncol 27:2046–2051
9. Banerjee S, Sengupta PS, Mukherjee AK (2010) Chem Phys Lett 487:108–115
10. Alberto ME, Lucas MFA, Pavelka M, Russo N (2009) J Phys Chem B 113:14473–14479
11. Pavelka M, Lucas MFA, Russo N (2007) Chem Eur J 13:10108–10116
12. Deubel DV (2006) J Am Chem Soc 128:1654–1663
13. Lau JKC, Deubel DV (2006) J Chem Theory Comput 2:103–106
14. Burda JV, Zeizinger M, Leszczynski J (2005) J Comp Chem 26:907–914
15. Robertazzi A, Platts JA (2004) J Comp Chem 25:1060–1067
16. Costa LAS, Rocha WR, De Almeida WB, Dos Santos HF (2004) Chem Phys Lett 387:182–187
17. Costa LAS, Rocha WR, De Almeida WB, Dos Santos HF (2003) J Chem Phys 118:10584–10592
18. Zhang Y, Guo ZJ, You XZ (2001) J Am Chem Soc 123:9378–9387
19. Carloni P, Sprik M, Andreoni W (2000) J Phys Chem B 104:823–835
20. Lopes JF, Rocha WR, Dos Santos HF, De Almeida WB (2008) J Chem Phys 128:165103
21. Baik MH, Friesner RA, Lippard SJ (2003) J Am Chem Soc 125:14082–14092
22. Spiegel K, Rothlisberger U, Carloni P (2004) J Phys Chem B 108:2699–2707
23. Robertazzi A, Platts JA (2006) Chem Eur J 12:5747–5756
24. Beret EC, Pappalardo RR, Marx D, Sánchez Marcos E (2009) Chem Phys Chem 10:1044–1052
25. Bouvet D, Michalowicz A, Crauste-Manciet S, Brossard D, Provost K (2006) Inorg Chem 45:3393–3398
26. Curis E, Provost K, Bouvet D, Nicolis I, Crauste-Manciet S, Brossard D, Bénazeth S (2001) J Synchrotron Radiat 8:716–718
27. Beret EC, Provost K, Muller D, Sánchez Marcos E (2009) J Phys Chem B 113:12343–12352
28. Chen Y, Guo ZJ, Parsons S, Sadler PJ (1998) Chem Eur J 4:672–676
29. Chen Y, Guo ZJ, Parkinson JA, Sadler PJ (1998) J Chem Soc Dalton Trans 3577–3585
30. Miller SE, House DA (1989) Inorg Chim Acta 161:131–137
31. Raber J, Chuanbao Z, Eriksson LA (2004) Mol Phys 102:2537–2544
32. Zhu CB, Raber J, Eriksson LA (2005) J Phys Chem B 109:12195–12205
33. Frisch MJ, Trucks GW, Schlegel HB, Scuseria GE, Robb MA, Cheeseman JR, Montgomery JA, Vreven T, Kudin KN, Burant JC, Millam JM, Iyengar SS, Tomasi J, Barone V, Mennucci B, Cossi M, Scalmani G, Rega N, Petersson GA, Nakatsuji H, Hada M, Ehara M, Toyota K, Fukuda R, Hasegawa J, Ishida M, Nakajima T, Honda Y, Kitao O, Nakai H, Klene M, Li X, Knox JE, Hratchian HP, Cross JB, Bakken V, Adamo C, Jaramillo J, Gomperts R, Stratmann RE, Yazyev O, Austin AJ, Cammi R, Pomelli C, Ochterski JW, Ayala PY, Morokuma K, Voth GA, Salvador P, Dannenberg JJ, Zakrzewski VG, Dapprich S, Daniels AD, Strain MC, Farkas O, Malick DK, Rabuck AD, Raghavachari K, Foresman JB, Ortiz JV, Cui Q, Baboul AG, Clifford S, Cioslowski J, Stefanov BB, Liu G, Liashenko A, Piskorz P, Komaromi I, Martin RL, Fox DJ, Keith T, Laham Al, Peng CY, Nanayakkara A, Challacombe M, Gill PMW, Johnson B, Chen W, Wong MW, Gonzalez C, Pople JA (2003) Gaussian 03, revision E.01
34. Adamo C, Barone V (1998) J Chem Phys 108:664–675
35. Andrae D, Haussermann U, Dolg M, Stoll H, Preuss H (1990) Theor Chim Acta 77:123–141
36. Burda JV, Zeizinger M, Sponer J, Leszczynski J (2000) J Chem Phys 113:2224
37. Cances E, Mennucci B, Tomasi J (1997) J Chem Phys 107:3032–3041
38. Rappe AK, Casewit CJ, Colwell KS, Goddard WA, Skiff WM (1992) J Am Chem Soc 114:10024–10035
39. Michalska D, Wysokin'ski R (2001) J Comp Chem 22:901–912
40. Raudaschl G, Lippert B, Hoeschele JD, Howard-Lock HE, Lock CJL, Pilon P (1985) Inorg Chim Acta 106:141–149
41. Battle AR, Choi R, Hibbs DE, Hambley TW (2006) Inorg Chem 45:6317–6322
42. Marcelis ATM, Van der Veer JL, Zwetsloot JCM, Reedijk J (1983) Inorg Chim Acta 78:195–203
43. Arnesano F, Natile G (2008) Pure Appl Chem 80:2715–2725
44. Kasparkova J, Vojtiskova M, Natile G, Brabec V (2008) Chem Eur J 14:1330–1341
45. Miller SE, House DA (1989) Inorg Chim Acta 166:189–197
46. Lopes JF, Menezes VSD, Duarte HA, Rocha WR, De Almeida WB, Dos Santos HF (2006) J Phys Chem B 110:12047–12054
47. Fu CF, Tian SX (2010) J Chem Phys 132:174507
48. Chen Y, Parkinson JA, Guo ZJ, Brown T, Sadler PJ (1999) Angew Chem Int Ed 38:2060–2063